Ann. Geophysicae 13, 494–504 (1995)

Annales Geophysicae

Energy dissipation during a small substorm

A. Belehaki[1], H. Mavromichalaki[2], D. V. Sarafopoulos[3], E. T. Sarris[1,3]

[1] Institute of Ionospheric and Space Research, National Observatory of Athens, Lofos Nymphon, Thission PO Box 20048, 11810 Athens, Greece
[2] Nuclear and Particle Physics Section, Physics Department, University of Athens, Solonos 104, 10680 Athens, Greece
[3] Demokritos University of Thrace, Department of Electrical Engineering, 67100 Xanthi, Greece

Received: 16 July 1992/Revised: 11 February 1994/Accepted 16 September 1994

Abstract. The relative importance of the two most likely modes of input energy dissipation during the substorm of 8 May 1986, with an onset at 12:15 UT (CDAW 9E event), is examined here. The combination of data from the interplanetary medium, the magnetotail and the ground allowed us, first of all, to establish the sequence of phenomena which compose this substorm. In order to calculate the magnetospheric energetics we have improved the Akasofu model, by adding two more terms for the total magnetospheric output energy. The first one represents the energy consumed for the substorm current wedge transformation, supplied by the asymmetric ring current. This was found to be 39% of the solar wind energy entering the magnetosphere from the start of the growth phase up to the end of the expansion phase. The second term represents the energy stored in the tail or returned to the solar wind. Our results suggest that the substorm leaves the magnetosphere in a lower energy state, since, according to our calculations, 23% of the energy that entered the magnetosphere during the whole disturbance was returned back to the solar wind. Finally, it is interesting to note that during the growth phase the driven system grow considerably, consuming 36% of the solar wind energy which entered the magnetosphere during this early phase of the substorm.

1 Introduction

The magnetosphere is a magnetohydrodynamic (MHD) dynamo which converts solar wind energy into electric current energy. The cross-tail current in the magnetotail is a resistive portion of the current solenoids driven by the MHD dynamo (Alfven, 1981). Since the substorm auroral electrojets are linked with magnetospheric currents, the near-Earth portion of the cross-tail current is interrupted and diverted into the ionosphere at the onset of magnetospheric substorms. At the synchronous distance and in the near-Earth magnetotail near the equatorial plane, magnetic field observations have indicated that the magnetosphere relaxes to a more dipolar field configuration during substorm expansion (McPherron *et al.*, 1973; Lui, 1978; Fairfield *et al.*, 1981; Kaufmann, 1987).

The energy that triggers the whole disturbance of a magnetospheric substorm is provided by the solar wind. Perreault and Akasofu (1978) have suggested an empirical formula which describes the input energy as a function of the interplanetary medium parameters. This formula has been used by many researchers to measure the input solar wind energy. Akasofu (1980) has studied the processes of energy input during magnetic storms. His results supported the idea that solar wind energy is directly converted into storm energy without intervening storage in the tail. The processes of direct input is probably important on longer time scales and during magnetic storms. Pytte *et al.* (1978) have distinguished between sudden onset substorms and periods of direct conversion of solar wind energy. Fairfield *et al.* (1981) in a detailed analysis have confirmed the importance of the magnetotail in supplying energy for sudden onset substorms. On the other hand they have noted cases of increasing tail energy density during some disturbances which indicate that direct dissipation, in the ionosphere, of solar wind energy is another mode of input. However, the direct mode of input cannot explain the explosive dissipation of energy at substorm onset.

Rostoker *et al.* (1987) have distinguished three physical processes in substorm disturbances: the driven process, the storage process and the release process. The driven process involves the direct deposition of energy in the inner magnetosphere and the dissipation of energy into the auroral ionosphere. The storage process involves the loading of the input energy into the magnetotail. The release process involves the sudden release (i.e. unloading) of the energy previously stored in the tail and its subsequent dissipation in the auroral ionosphere or injection back to the solar wind.

Correspondence to: A. Belehaki

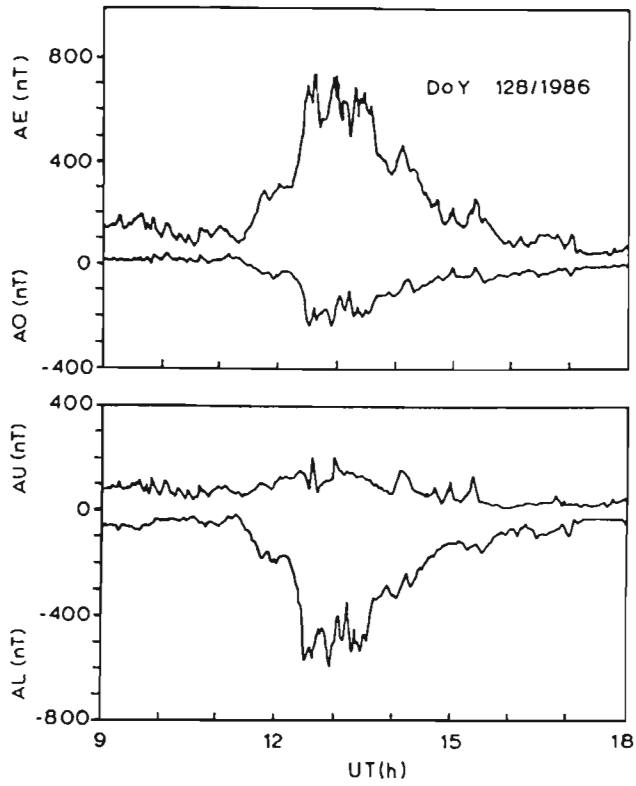

Fig. 1. Time plots of the 1-min values of the auroral electrojet indices AL, AU, AO and AE for the substorm of 8 May 1986 between 09:00 UT and 18:00 UT

The aim of this work is to study substorm energy transformation modes and to determine the relative magnitude of the competing processes during a substorm of weak solar wind coupling (i.e. low input power) with onset at 12:15 UT on 8 May 1986. This event has previously been studied as part of CDAW 9E. McPherron *et al.* (1990) and McPherron (1991) presented a correlation study between ground observations and magnetotail data. They concluded that there is evidence of a near-Earth neutral line formation and established that the CDAW 9E event is a typical example of close correlation between phenomena on the Earth's surface and the near-magnetotail plasma sheet. The same conclusion was reported by Saifudinova *et al.* (1992, and references therein), using the magnetogram inversion technique (MIT) to calculate various electrodynamic parameters of the Earth's magnetosphere. Mavromichalaki and Belehaki (1993) have analysed the magnetospheric energy budget during this event, using both the models of Akasofu (1981) and that of Vasyliunas (1987), taking into consideration the energy variations in the magnetotail. They concluded that the driven system increased considerably while a weaker unloading event was superposed at the onset of the expansion phase.

The model which we follow in this paper is based on the Akasofu method (1981) of computing the magnetospheric energy budget. In order to fit the Akasofu equations to the CDWA 9E event, which is an isolated substorm of weak solar wind coupling, we introduce some necessary corrections to estimate the symmetric ring current injection rate. Moreover, we propose an empirical formula for the rate of energy dissipation in the substorm current wedge formation (supplied by the asymmetric ring current) and for the rate of energy return from the magnetosphere to the solar wind.

2 Ground signatures

2.1 Auroral electrojet indices

The auroral electrojet indices data used here were obtained from the 1-min values of the H-component from 11 geomagnetic stations located along the auroral oval. These data were provided by the WDC-C2 Center for Geomagnetism and are part of the PROMIS data base.

Table 1. The coordinates of the magnetic observatories referred to in this study

Station	Abbreviation	Geographic coordinates		Geomagnetic coordinates	
		Latitude (degrees)	Longitude	Latitude (degrees)	Longitude
Baker Lake	BLC	64.4	264.0	72.9	318.7
Inuwik	INK	68.3	226.7	70.9	264.8
Yellowknife	YEK	62.4	245.6	69.6	294.1
Barrow	BRW	71.3	203.3	71.7	236.0
Fort Simpson	FSP	61.7	238.8	68.2	291.1
Fort Smith	FSM	60.0	248.0	67.4	298.9
Fort Yukon	FYU	66.6	214.7	69.2	253.8
College	COL	64.9	212.0	66.9	252.9
Meanook	MEA	54.6	246.7	61.9	299.6
Anchorage	ANC	61.2	210.1	63.3	254.0
Sitka	SIT	57.1	224.7	61.6	272.6
Tucson	TUC	32.3	249.2	39.9	311.4
San Juan	SJG	18.1	293.9	29.6	3.1
Kakioka	KAK	36.2	140.2	26.0	206.0
Honolulu	HON	21.3	202.0	21.1	266.5

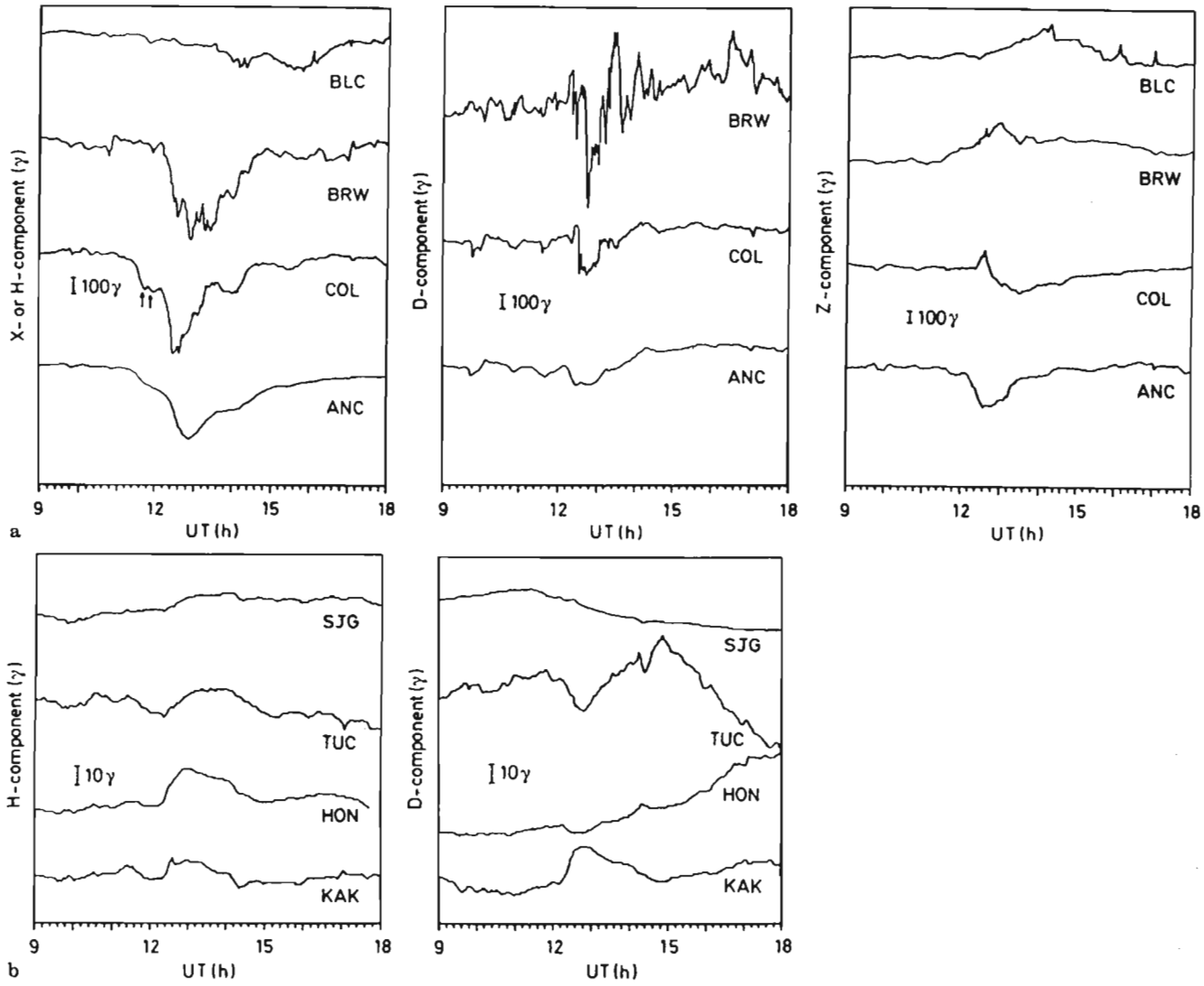

Fig. 2a. Time plots of the 1-min values of the X- or H-components (left), D-component (center) and Z-component (right) from the observatories Baker Lake, Barrow, College and Anchorage located in the low polar cap and in the auroral oval. **b** Time plots of the 1-min values of the H-component (left) and of the D-component (right) from the low-latitude observatories San Juan, Tucson, Honolulu and Kakioka

The variations in the AE- and AO-indices from 09:00 UT to 18:00 UT on 8 May 1986 are given in the top panel of Fig. 1, whilst the variations in the AL- and AU-indices are shown in the lower panel of the same figure. A first decrease in the AL-index is clearly observed around 11:30 UT, but at 12:15 UT a second sharp decrease is detected.

2.2 Ground magnetograms

To obtain a picture of the substorm signature on the ground we have examined the ground magnetograms from the auroral oval, polar cap and low-latitude stations. These data are also part of the PROMIS data base. The geographic and the geomagnetic coordinates of the stations used here are given in Table 1. The time plots of the geomagnetic field H-, D-, and Z-components from four selected auroral oval and polar cap stations are presented in Fig. 2a. The time plots of the H- and D-components from the low-latitude stations are presented in Fig. 2b, since the Z-component at low-latitude is negligible.

From the magnetograms of the auroral observatories Anchorage and College (Fig. 2a, left panel), we can observe, prior to the main substorm an initial variation in the H-component between 11:15 UT and 12:15 UT. The magnetogram of the H-component from College shows two successive excursions at 11:40 UT and 11:52 UT (indicated with arrows in Fig. 2a), which occur before the main onset. These events may be characterised as pseudobreakups that occur during the growth phase of the substorm. Note that the H-component magnetogram from Barrow, which is a low polar cup station, does not show any initial variation between 11:15 UT and 12:15 UT, although a very large negative bay appeared after 12:15 UT.

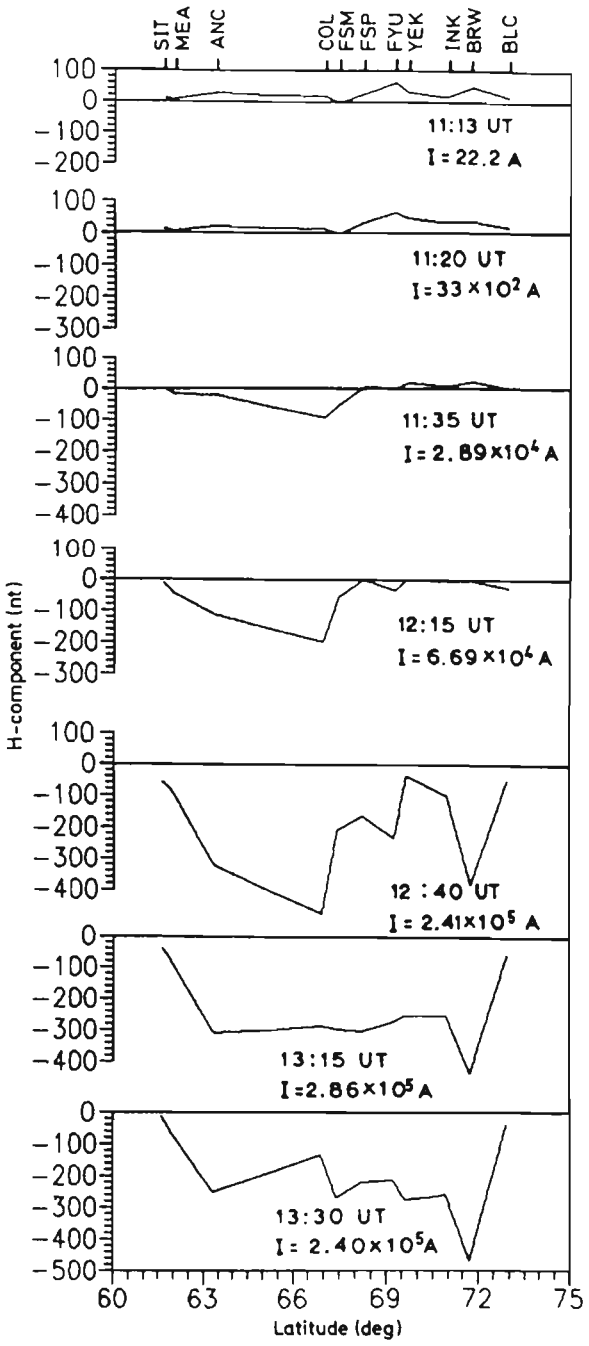

Fig. 3. The latitudinal profiles of the H-component variations along the chain of the stations noted in the top panel at several time epochs of the substorm occurred on 8 May 1986

The latitudinal profile of the H-component at various times in the substorm and the total current of the westward electrojet flowing across the chain of the high-latitude stations of Table 1 is presented in Fig. 3. The current intensity was calculated using Ampere's law, assuming that the horizontal magnetic variation is produced by an overhead electric current. The maximum value of the westward electrojet current at the expansion phase is in the order of 10^5 A. This is about one order of magnitude smaller than that for typical substorms (Kamide and Akasofu, 1974). The center of the electrojet shifts equatorward as the total current intensity increases (Fig. 3 see the three last panels). There is also a tendency for the latitudinal width to increase for greater values of the current intensity (compare in Fig. 3 the profiles at 12:15 UT, 12:40 UT and 13:15 UT). From 12:40 UT to 13:15 UT, where the AE-index reaches a maximum, the intensity of the westward electrojet is also maximized. This demonstrates that the westward electrojet intensity is proportional to the AE-index. After 13:30 UT the current intensity decreased, which means that the substorm recovery had started, and it was accompanied by the poleward shifting of the westward electrojet.

For the low-latitude station magnetograms, plotted in Fig. 2b, the positive variations detected in the H-component are due to the integrated effects of the substorm current wedge (Kokubun and McPherron, 1981). Each positive H-bay is accompanied by a westward deflection of the field (negative D perturbation) at the Honolulu and Tucson stations. This indicates that both stations were east of the center of the current wedge (Rostoker *et al.*, 1980) in a region where the net field-aligned current (FAC) was earthward (Nagai, 1982), that is in the postmidnight sector. In contrast, the eastward deflection of the field (positive D perturbation) at Kakioka indicates that the observatory was to the west of the western edge of the substorm-disturbed region. The San Juan observatory was located in the dayside magnetosphere and so was not affected by the FAC.

3 Interplanetary medium data

The interplanetary magnetic field and the solar wind plasma measurements were obtained from the IMP-8 spacecraft which was launched in a circular geocentric orbit of $\approx 35\ R_E$ in October 1973. The magnetic field data have a time resolution of 15.336 s, whilst the plasma data represent averages of 1 min. IMP-8 was located at $Xse = 37R_E$ and $Yse = 4R_E$, at 11:00 UT. This results in an estimated time delay equal to (7 ± 2) min between the IMP-8 and the Earth's magnetosphere (the solar wind bulk speed has been taken as equal to 420 km s^{-1}). Time plots of these interplanetary data are presented in Fig. 4.

After an interval of variable but mostly northward direction, the IMF returns to a southward orientation at 11:13 UT. From Fig. 4 it is obvious that this was associated with a large discontinuity which is apparent in the other two components of the interplanetary magnetic field (IMF). The sudden northward turning of the IMF *Bz*-component at 11:35 UT may have triggered the initial intensification of the westward electrojet denoted by the preliminary decrease of the H-component at some auroral observatories. Nevertheless, the southward turning of the IMF does not appear to have produced the main onset of the expansion phase, since this occurred at 11:13 UT, whilst the expansion onset occurred at 12:15 UT (i.e. the growth phase lasts almost 1 h).

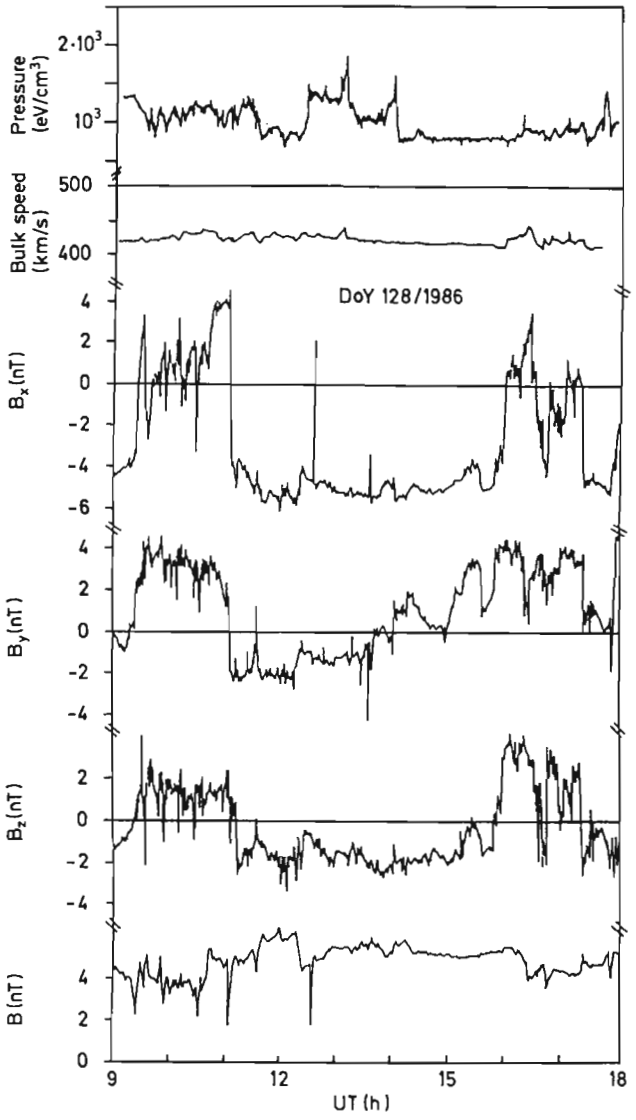

Fig. 4. The solar wind dynamic pressure, bulk speed V, the B_x-, B_y-, and B_z-components in SE coordinates and the IMF magnitude B, for the period between 09:00 UT and 18:00 UT of 8 May 1986 measured by IMP-8 spacecraft

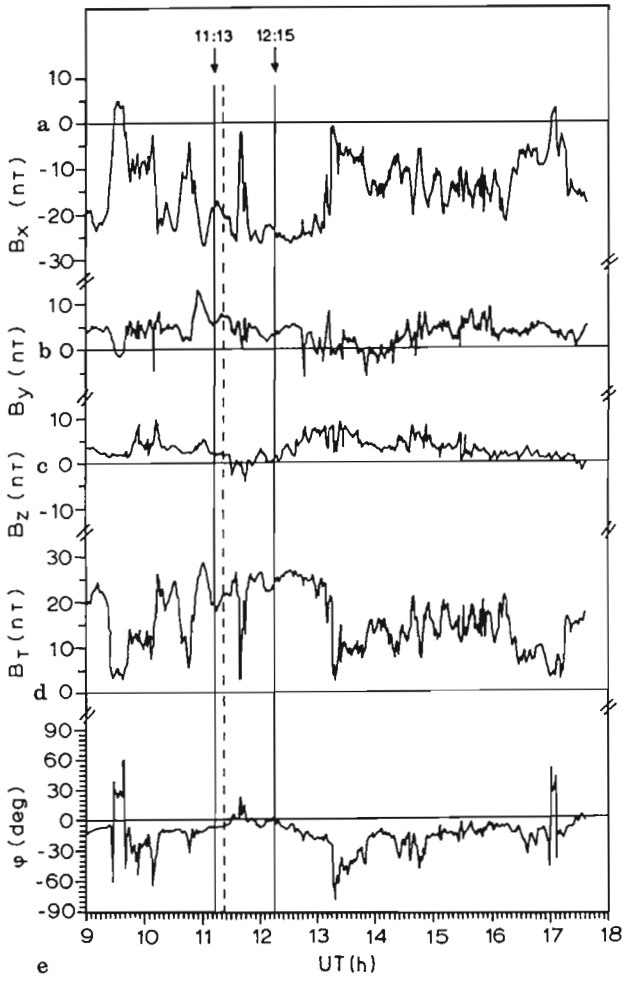

Fig. 5a–e. Time plots of the B_x-, B_y-, B_z-components and of the magnitude B_T of the tail magnetic field, measured by ISEE-1 spacecraft in SM coordinates for the substorm examined here, together with the variations of the angle φ as determined in the text

4 Magnetotail morphology

Significant changes occur in the near-Earth magnetotail during a magnetospheric substorm. McPherron *et al.* (1973) found that during substorms there are very large changes in the magnetic field configuration in this region. These changes are systematically related to the onset of the expansion phase identified with ground magnetograms. During the growth phase the magnitude of the tail field increases and its orientation becomes more tail-like. In the expansion phase the magnitude decreases and the field orientation becomes more dipolar. These changes suggest that energy stored in the tail during the growth phase is released in the expansion phase, leaving the tail in a lower energy state after the substorm (Fairfield and Ness, 1970).

In order to study the state of the tail prior to or during the early phases of the substorm examined here, we have used the particle flux data and the magnetic field data measured from the ISEE-1 spacecraft. ISEE-1 was launched on 22 October 1977 into a highly elliptical orbit. Measurements of the magnetic field were provided by the UCLA fluxgate magnetometer on ISEE-1 (Russell, 1978).

The three components *Bx*, *By* and *Bz* of the tail magnetic field in solar magnetospheric coordinates (SM), together with the total field magnitude B_T, are shown in panels a, b, c and d, respectively of Fig. 5. The times of southward turning and of the onset are marked on Fig. 5. ISEE-1 was located south of the neutral sheet since $Bx < 0$. The effect of the total field magnitude decrease detected from 12:40 UT to 13:15 UT is primarily due to the large decrease in |Bx| component. This was first reported by Camidge and Rostoker (1970) to be the predominant effect on the tail in substorm disturbances. During the growth phase of the substorm in the magnetotail, between 11:20 UT and 12:15 UT, the *Bz*-component of the tail field shows some variation near zero and just before the expansion onset, *Bz* was almost zero. At this time |Bx| was larger than 25γ. Consequently, the field orientation was essentially parallel to the neutral sheet.

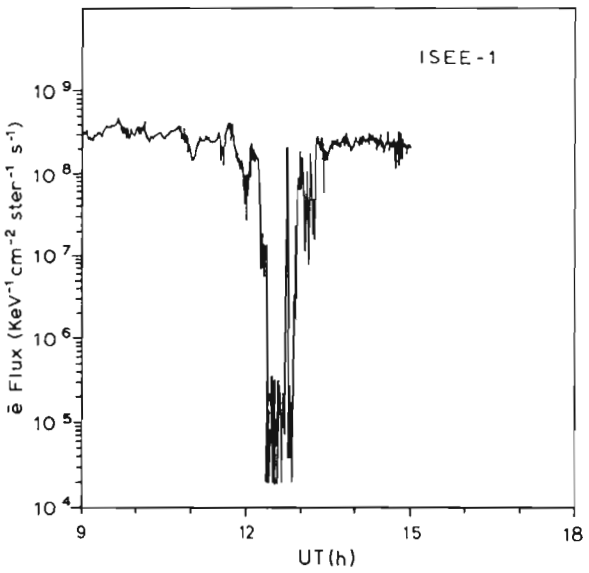

Fig. 6. The 6-keV electron flux measured by ISEE-1 spacecraft with a 4-s resolution, for the period examined here

Such an orientation is typical for the tail lobe or plasma sheet boundary layer. The start of the increase in the *Bz*-component and the decrease in |Bx| appear to be associated with the onset of the expansion phase at 12:15 UT. These changes indicate a rapid rotation of the field from tail-like to a more dipole-like configuration. Therefore, in order to determine more precisely the time of rotation of the field from a tail-like to a more dipole-like shape, we plotted the angle φ, which is the angle between the projection of the field's vector in the XZ-plane and the equatorial plane. The time plot of the angle φ is shown in Fig. 5e. It is obvious that just after the expansion onset the magnitude of the angle φ starts to increase which means that the field rotates to a more dipolar configuration. This angle becomes generally small during substorm growth and is almost zero for some minutes before the onset. This means that just before the onset the field's configuration was extremely tail-like. At 12:40 UT, when the AE-index obtained its maximum value, B_T began a rapid decrease lasting until 13:15 UT. This decrease was accompanied by a rapid increase in the *Bz*-component of the tail field.

The low-energy 6-keV electron flux data plotted in Fig. 6 were obtained by the particle detector of Anderson *et al.* (1978) on ISEE-1 (the Berkeley-Seattle-Toulouse experiment). The detector looks southward parallel to the satellite spain axis (i.e. normal to the ecliptic plane). These electrons are representative of the plasma sheet plasma and the plot is particularly useful in identifying the dropout and recovery of the plasma sheet (beyond 12–15 R_E), which often marks the occurrence of substorms. At 11:30 UT, ISEE-1 was located south of the neutral sheet at $X = -20\ R_E$ at 23:30 LT. The electron flux data (Fig. 6) indicate that ISEE-1 was initially located in the plasma sheet boundary layer since the energy flux was greater than $10^8\ keV^{-1}cm^{-2}sr^{-1}s^{-1}$ and $Bx < 0$. The plasma sheet dropout at 6 keV began at 12:12 UT. At 12:22 UT the plasma sheet vanished, leaving the spacecraft in the south lobe. The plasma sheet remained very thin for about 30 min, whilst negative magnetic bays persisted at auroral latitudes. At 12:52 UT the plasma sheet began expanding over the spacecraft which after this time had therefore returned to the central plasma sheet.

The major substorm intensification took place at 12:40 UT (Figs. 1 and 2) when the auroral electrojets are thought to be fed by the disrupted cross-tail current. The negative magnetic bays at auroral latitudes started to recover after the plasma sheet thickening, and bays at low polar cap latitudes begin to appear as shown, for example, by the X-magnetogram of the Baker Lake (BLC) station presented in Fig. 2a. This is due to the poleward shifting of the westward electrojet. This effect probably results from the initiation of the field line merging at a new location in the magnetotail, far beyond the ISEE-1 position (Hones *et al.*, 1973). All these elements provide a clear example of the close correlation between phenomena on the Earth's surface and the near-magnetotail's plasma sheet, as has also been reported by McPherron (1991) and McPherron *et al.* (1990).

In summary, the sequence of the phenomena which compose this substorm have been established as follows.

The beginning of the growth phase in the tail corresponds closely to the appearance of a southward component of the interplanetary magnetic field (IMF). This reaches the magnetopause at 11:20 UT and it is detected at IMP-8 position at 11:13 UT. Just before the expansion onset ISEE-1, at $20\ R_E$ downstream, detects (a) an increase of the field magnitude in the lobe of the tail, (b) a decrease in *Bz*-component of the tail field, (c) the development of a tail-like field configuration and (d) a thinning in the plasma sheet.

Immediately after the onset of the expansion phase the magnitude of the angle φ began to decrease and the field started to rotate slowly to a more dipole-like configuration.

5 Energy consideration for the 8 May 1986 substorm

In order to determine the mechanisms by which the energy input is dissipated in the magnetosphere, we have studied the energy budget of the magnetosphere during this isolated substorm. In the following, we assume that the rate of the solar wind energy input into the magnetosphere is expressed by the solar wind-magnetosphere coupling parameter ε, proposed by Perreault and Akasofu (1978):

$$\varepsilon = V \cdot B^2 \cdot \sin^4\left(\frac{\theta}{2}\right) \cdot l_o^2, \quad \text{erg s}^{-1}, \tag{1}$$

where, B is the magnitude of the IMF, V is the solar wind bulk speed, θ is given by $\tan^{-1}(B_y/B_z)$ or by the angle's supplement for $B_z < 0$ and l_o^2 is an effective cross-sectional area of the magnetosphere, where l_o denotes the linear dimension of the cross-sectional area. Kan and Akasofu (1974) showed that the value of the distance l_o can only be appreciably affected during periods when IMF has an

extraordinarily large southward component. In cases of weak solar wind-magnetosphere coupling, the distance l_o can be considered constant as a first approximation. As to the numerical value of l_o, this has been chosen by Akasofu (1981) to be equal to 7 Earth radii (R_E) and corresponds to the combination of $R_T \approx 2r_N$ and $L_T \approx 8r_N$, where R_T is the radius of the tail, L_T is the effective width of the tail current sheet and r_N is the geocentric distance of the neutral line. We consider the value of $7R_E$ for the l_o to be a reasonable order of magnitude. Moreover, to our knowledge a value for l_o greater than $8R_E$ has never been used in the literature.

The energy input is not immediately dissipated within the ionosphere and experiences a series of transformations. Following the Akasofu model (Akasofu, 1981), the magnetosphere dissipates the input solar wind energy into the ionosphere and the symmetric ring current with the driven process. So, the total energy consumption rate of the magnetosphere, U_T, is given by the sum of the kinetic power of the auroral particles U_A, being lost in the ionosphere due to the collision, of the Joule heating U_J, associated with electric current flow in the resistive ionosphere and of the rate of injection of energy in the ring currents U_{RC}, flowing the magnetospheric equatorial plane and the neutral sheet, given by the equations:

$$U_A = \mathrm{AE} \times 10^{15}, \quad \mathrm{erg\,s^{-1}}, \tag{2}$$

$$U_J = 2 \times 10^{15}\,\mathrm{AE}, \quad \mathrm{erg\,s^{-1}}, \tag{3}$$

$$U_{RC} = 4 \times 10^{20}\left(\frac{dD_{st}}{dt} + \frac{D_{st}}{\tau_s}\right), \quad \mathrm{erg\,s^{-1}}, \tag{4}$$

where τ_s is the lifetime of the symmetric ring current particles. So, we can write

$$U_T = U_A + U_J + U_{RC}. \tag{5}$$

In the present study, we try to determine a more realistic function for the output magnetospheric energy U_T. Thus we introduce the following improvements to the Akasofu (1981) model (Eq. 5).

Firstly, we assume that during the whole process the lifetime of the symmetric ring current particles remains constant. Indeed, Zwickl *et al.* (1987) have shown that when τ_s is a multistep function of ε, the output energy U_T contains some unphysical step-like changes, whenever a new τ_s step is encountered. When τ_s is a continuous function of ε, the energy U_T shows a very obvious correlation with ε, and therefore it is not surprising that U_T and ε are highly correlated in Akasofu's (1981) study. U_T derived with a constant τ_s shows no evident correlation. The substorm examined here is produced by weak solar wind coupling ($D_{st} > -30\,\gamma$, $\varepsilon < 10^{18}\,\mathrm{erg\,s^{-1}}$), therefore we can set the time τ_s equal to 20 h, since Akasofu's theory predicts the same value for the lifetime of the ring current particles when $\varepsilon < 10^{18}\,\mathrm{erg\,s^{-1}}$ (Akasofu, 1981).

Moreover, in order to compute the symmetric ring current energy injection rate in the Akasofu's empirical formula (Akasofu, 1981), we have substituted the disturbed values of the H-component from the San Juan observatory for the D_{st} index. This observatory is a low-latitude station located in the dayside magnetosphere (07:00 LT) at the expansion onset of this event. Therefore, San Juan is primarily subjected to the symmetric ring current response. This substitution provides us with a high-resolution proxy for D_{st} as long as San Juan is not affected by the asymmetric ring current.

According to the above-mentioned improvements, the ring current energy injection rate (Eq. 4) can be corrected using the following equation:

$$U_{RC} = 4 \times 10^{20}\left(\frac{d\bar{H}_D}{dt} + \frac{\bar{H}_D}{\tau_s}\right), \quad \mathrm{erg\,s^{-1}}, \tag{6}$$

where $\bar{H}_D$ (for dayside) denotes the 1-min values of the pressure-corrected disturbed values of the H-component from the San Juan observatory defined by Burton *et al.* (1975):

$$\bar{H}_D = |H_D| - H_D(P),$$

where

$$H_D(P) = aP^{1/2} - b,$$

with $a = 0.2\,\mathrm{nT/(eV\,cm^{-3})^{1/2}}$, $b = 20\,\mathrm{nT}$, P is the solar wind dynamic pressure presented in the top panel of Fig. 4 and H_D the disturbed values of the H-component from the San Juan observatory.

Our next improvement concerns the tail energy variations. As we have shown in the previous section, the magnetosphere evolves from tail-like to a dipolar-like configuration after the onset of the expansion phase. The dipolarization of the field is due to the cross-tail current disruption which drives the FAC. The Honolulu magnetic observatory is subjected to the magnetic field of both the symmetric and asymmetric ring current, as it was located at 01:00 LT at the onset of the expansion phase of this event. The asymmetric ring current is part of an outer ring current whose nightside portion forms part of the cross-tail current in the magnetotail. At the onset of the expansion phase, the energy previously stored in the asymmetric ring current is dissipated in the formation of the substorm current wedge. Therefore, in order to estimate the energy consumption rate in the inner magnetosphere, as supplied by the asymmetric ring current, the following equation may be used:

$$U_{RC,AS} = 4 \times 10^{20}\left(\frac{dH_N}{dt} - \frac{d\bar{H}_D}{dt} + \frac{H_N}{\tau_A} - \frac{\bar{H}_D}{\tau_s}\right), \quad \mathrm{erg\,s^{-1}}, \tag{7}$$

where, τ_A is the mean lifetime of the particles which compose the asymmetric ring current, taken as equal to 2 h (Clauer *et al.*, 1983) and H_N denotes the 1-min disturbed values of the H-component from the Honolulu observatory multiplied by a correction factor equal to 2/3. This factor accounts for the effect of an induced current within the Earth's interior, i.e. we have assumed that the contribution from the ionospheric current to the observed geomagnetic perturbation is twice that of the current flowing above the Earth (Kamide and Akasofu, 1974; Rostoker, 1991, personal communication).

Finally, it is known that the tail energy changes during a substorm disturbance. Fairfield *et al.* (1981) have confirmed the importance of the tail storage in producing

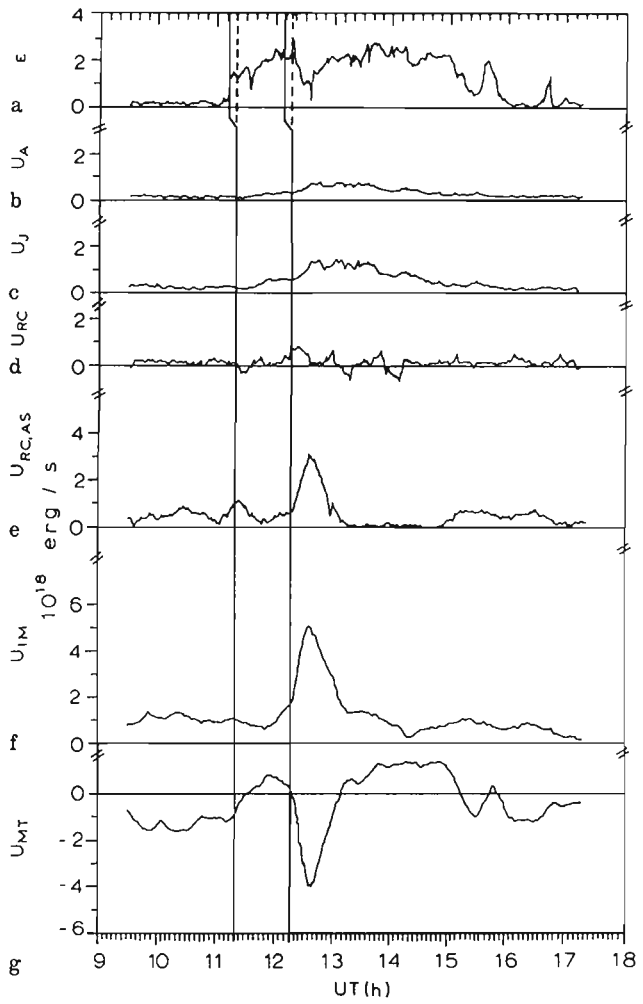

Fig. 7a–g. The time plots of the power functions ε, U_A, U_J, U_{RC}, $U_{RC,AS}$, U_{IM}, and U_{MT} estimated for the event studied here, computed according to Eqs. (1), (2), (3), (6), (7), (9) and (8), respectively, assuming that the tail cross-section is equal to $(7R_E)^2$

substorms. Whether the tail energy increases or decreases will depend on the relative magnitude of the two competing processes, that is the storage process and the unloading process. Therefore, in order to have a measure of the amount of energy stored or released from the tail, U_{MT}, we have substracted the sum of the values U_A, U_J, U_{RC}, and $U_{RC,AS}$ from the corresponding values of the input energy ε, using a time delay τ_d equal to 7 min (see the section about the interplanetary medium data):

$$U_{MT}(t) = \varepsilon(t - \tau_d) - U_{IM}(t), \tag{8}$$

where

$$U_{IM}(t) = U_A(t) + U_J(t) + U_{RC}(t) + U_{RC,AS}(t). \tag{9}$$

The time plots of the energy rate functions ε, U_A, U_J, U_{RC}, $U_{RC,AS}$ and U_{MT} estimated for the event examined here are given in Fig. 7. The southward turning of the IMF at 11:13 UT results in the immediate increase of the energy input ε. At 11:20 UT the energy that remains in the magnetotail increases, i.e. the input solar wind energy is immediately stored in the tail. This storage can be thought of as applying both to the magnetotail currents and to the asymmetric current. This is in accordance with our real data (Fig. 5e), as during the growth phase the angle φ takes very small values, which means that the magnetosphere is close to a tail-like configuration and therefore the power U_{MT} which is stored in the tail goes into the cross-tail currents enhancement. However, after 11:35 UT, the energy dissipation rates U_A and U_J, presented in Fig. 7b and c respectively, are slowly increased, indicating that a part of the input energy has been converted directly into driving the auroral electrojets.

In summary, from the start of the substorm at 11:13 UT until 11:35 UT, the input solar wind energy is stored directly into the tail. From 11:35 UT to 12:15 UT, a part of the input energy is dissipated from growth of the driven system, whilst the rest of the input energy is stored continuously into the tail.

At 12:15 UT the energy stored in the tail during the growth phase was dissipated explosively in the inner magnetosphere-ionosphere according to the following sequence. First of all, the $U_{RC,AS}$ energy rate increased sharply immediately after the onset, indicating the activation of substorm current wedges in the midnight sector. The U_A and U_J energy rates increased more rapidly after 12:15 UT, indicating that from this moment the auroral electrojets are fed by the FAC. This explosive dissipation of the tail energy shows that the unloading process is the dominant mode of energy dissipation at the expansion onset. Finally, we must note that the symmetric ring current injection rate U_{RC} was not considerable since the level of the U_{RC} after the onset did not exceed the U_{RC} level during the quiet period before the growth phase. This is expected since the magnetosphere was in the recovery phase of a large magnetic storm initiated on 6 May 1986 at $\approx$04:00 UT. The energy deposited into the symmetric ring current during this episode (for which power input from the solar wind to the magnetosphere was very large) was dissipated in the magnetosphere by the end of the day prior to that studied here (i.e. the end of 7 May 1986).

In order to have a more quantitative view of the energy balance, we have computed the time integrals of the energy rates whose time plots appeared in Fig. 7. During the growth phase we estimate that 64% of the input energy (5.8×10^{21} erg) was stored in the tail, while 36% was used for growth of the driven system electrojets. This fact supports the idea that the tail is an important source of the energy that triggers the substorm expansion onset. At the expansion onset, the energy released from the asymmetric ring current increases drastically and we estimated that at the end of the expansion phase the total energy released from the asymmetric ring current is equal to 5.5×10^{21} erg. This represents 39% of the total solar wind energy entering the magnetosphere from the beginning of the substorm to the end of the expansion phase. Moreover, from the time integral of the term U_{MT}, we estimated that the total energy ejected from the tail back to the solar wind during the whole disturbance was equal to 5.8×10^{21} erg, which represents 23% of the total input solar wind energy during the substorm interval. It should be remembered that throughout our analysis we have assumed that the cross-sectional area of the magnetotail

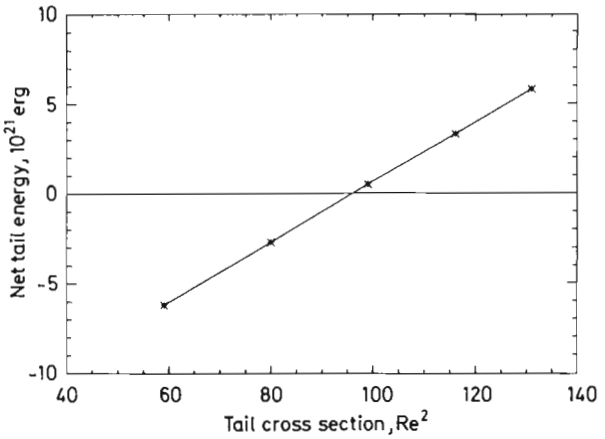

Fig. 8. The plot of the net energy remaining in the tail after the end of the substorm versus the tail cross-section. Note that for $l_o^2 = (9.4\ R_E)^2$ the substorm returns the magnetosphere to its initial energy state

lo^2 remains constant at $(7R_E)^2$ during the whole substorm disturbance. Based on this assumption, we concluded that the substorm leaves the magnetosphere in a lower energy state. To test how the choice of this particular value for the lo^2 parameter affects the above conclusion, we repeated our calculations for four other area factors. In Fig. 8, we present the plot of the net energy remaining in the tail versus different area factors lo^2. From this plot we estimate that lo^2 should be equal to $(9.4\ R_E)^2$ for the magnetosphere to return to its original state after the substorm is over. For values smaller than this, the magnetosphere is found to be in a lower energy state at the end of the substorm. We consider the numerical value of 9.4 R_E for l_o as very large since it represents the 180% of the original value of the tail cross section, proposed by Akasofu (1981) and extensively used in the literature to date.

For the above reasons, we think that our conclusion that the magnetosphere ends up in a lower energy state after this substorm is not artificial and does not originate from the adoption of a particular numerical value for the area factor.

6 Discussion and summary

During substorm disturbances the magnetotail experiences dynamic changes. It is agreed that the most dramatic portion of a magnetospheric substorm occurs at the onset of the expansion phase when the cross-tail currents are diverted through the auroral ionosphere. This explosive dissipation of substorm energy at the expansion onset is a consequence of the release of tail energy stored during the growth phase.

In this work, we have generally regarded the magnetotail as an energy reservoir, whose input is controlled by the IMF and from which energy is lost to the ionosphere, to the inner magnetosphere and perhaps to the solar wind. A southward IMF enhances the role of input solar wind energy to the magnetotail. During the growth phase the tail size increases and this is manifested in the ionosphere as an equatorward movement of the polar boundary, as shown in Fig. 3. Throughout this analysis we assumed that the cross-sectional area of the magnetotail is equal to $(7R_E)^2$, as originally proposed by Akasofu (1981). The tail magnetic field shows a more stressed configuration, as is obvious from the variations of the angle φ (Fig. 5e). These changes reflect the build-up of a strong cross-tail current in the midnight sector, detected at 20 R_E downstream. The same feature has been observed to occur during the growth phase in the near-Earth region, typically at 7 to 15 R_E downstream (Hones et al., 1984; Lopez and Lui, 1990; Lui *et al.*, 1988; Sauvaud and Winckler, 1980). This may be due to the predominance of the parallel component of the pressure and the increase in the field curvature as suggested by Kauffman (1987) and by Lui *et al.* (1988).

The enhanced dynamo during the growth phase (Fig. 7a), described by the parameter ε must increase both the cross-tail current and the region I FAC. This gives rise to pre-break-up auroral arcs (Lui, 1991), clearly observed during this substorm at the College observatory at 11:40 UT and at 11:52 UT. At the onset of the expansion phase the strong cross-tail current, produced during the growth phase, is suddenly drastically reduced. The diverted current flows along the pre-existing auroral arcs because they provide better conductivity channels. Auroral break-up probably occurs on one of the pre-existing arcs. In the longitudinal sector of the break-up, the removal of the intense cross-tail current and the creation of a loop through the ionosphere cause a sudden relaxation of a stretched magnetic field. This produces an earthward convection surge, whereby the stretched magnetic field line becomes more dipolar-like (Lui, 1991). It is interesting to note that our model shows with good time resolution that the energy released from the asymmetric ring current (computed by the $\int U_{RC,AS}\ dt$) increases drastically just after the expansion onset. Plasma tailward of the current disruption region is partially evacuated by the convection surge which results in a rarefaction wave propagating mainly down the tail at speeds up to the magnetosonic speed of several hundred kilometres per second (Chao *et al.*, 1977; Kropotkin, 1972). This leads to a thinning of the mid-tail plasma sheet (Lui, 1991) observed at 12:15 UT by ISEE-1 at 20 R_E downstream (Fig. 6).

In order to adjust the Akasofu model to our isolated substorm with weak solar wind coupling, we have taken the lifetime τ_s of the symmetric ring current particles to be constant at 20 h during the whole substorm disturbance (Zwickl *et al.*, 1987). Moreover, by substituting the normalized and pressure-corrected values of the H-component disturbance from a low-latitude observatory located in the dayside magnetosphere for the D_{st}-index, we have isolated the contributions of the symmetric ring current. The present D_{st}-index, due to the scarcity of stations from which it is computed, cannot distinguish between contributions from the symmetric ring current (containing energy deposited during the development of the substorm) and the asymmetric ring current (containing energy which is eventually deposited during the decay of the driven system), as was pointed out by Rostoker *et al.* (1987). Each of these currents has quite different time constants, with the decay of the storm-time ring current requiring several

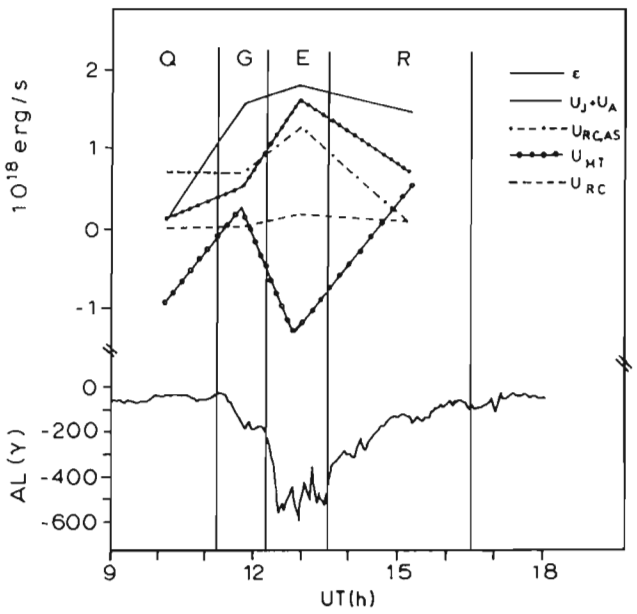

Fig. 9. The mean energy rate of the functions ε, U_{RC}, $U_A + U_J$, $U_{RC,AS}$, and U_{MT} during the quiet pre-substorm period (Q), the growth phase (G), the expansion phase (E) and the recovery phase (R) are shown together with the values of the AL-index for the event studied here

tens of hours and the decay of the asymmetric ring current requiring at most 2–4 h.

The third and fourth improvements are the most interesting and concern the calculation of the energy requirements in triggering the several dynamic processes observed in the magnetotail leading up to and following the expansion onset. It is important to distinguish the difference in meaning between the terms $U_{RC,AS}$ and U_{MT} used in the present model. The integral of the first over time describes the energy dissipated for the formation of the substorm current wedge which is supplied by the asymmetric ring current disruption. The integral of the second term over time estimates both the energy stored in the magnetotail during the storage process of the substorm (which consequently is transformed to $\int U_{RC,AS}\,dt$ energy during the decay of the driven system) and the energy which is ejected back to the solar wind during the release process, that is tailward of the cross-tail current disruption region.

The mean rate of the power ε, U_{RC}, $U_A + U_J$, $U_{RC,AS}$ and U_{MT} in 10^{18} erg s^{-1} during the quiet period before the substorm (Q) and during the growth (G), the expansion (E) and the recovery (R) phase are shown in Fig. 9. Our calculations were based on the assumption that $l_o = 7R_E$. The variations in $U_A + U_J$, $U_{RC,AS}$ and U_{MT} represent the unloading component of the magnetospheric response. The abrupt increase or decrease of the above quantities during the expansion phase clearly shows the predominance of the unloading process.

Mavromichalaki and Belehaki (1993) have examined the energy budget of the same substorm event using the methods of Akasofu (1981) and Vasyliunas (1987). In order to determine a better function for the total magnetospheric energy output U_T, they estimated the energy rate U_{MT} as the residual of the input power, calculated from the epsilon parameter, from the sum of the power dissipated in the ionosphere $U_A + U_J$ and the ring current U_{RC} for each minute of this substorm. The Akasofu model showed that the predominant mode of energy transfer and dissipation is the directly driven process, whilst a small amount of the input energy dissipated explosively at the expansion onset. Nevertheless, application of the Akasofu method to the real data did not clearly determine unloading events. In contrast, calculation of the magnetospheric energy budget using the Vasyliunas method (where the values of the output magnetospheric energy are independent of the solar wind energy input ε), showed more clearly that the unloading process took place at the onset of the expansion phase of this substorm. However, the lifetime of the symmetric ring current particles according to the Vasyliunas model was too small to fit with the weak solar-wind-coupling character of this event ($\varepsilon < 3 \times 10^{18}$ erg s^{-1}, $|D_{st}| < 30\,\gamma$).

The improved energy function for the total magnetospheric output energy proposed in this work has provided more realistic results in the energy considerations of the substorm examined.

1. The importance of the magnetotail in supplying the energy for the sudden onset at 12:15 UT was established.
2. More than one third of the input solar wind energy was explosively dissipated at 12:15 UT for the diversion of the cross-tail currents to the ionosphere.
3. The tail energy changed during this substorm. The rate of energy stored in the tail reached a minimum at 12:40 UT (Fig. 7g) when the ionospheric currents drained the tail of much of its energy since AE was at a maximum. Of the total input energy during the event 23% was returned to the solar wind, indicating that the tail was in a lower energy state at the end of the substorm expansion.
4. Apart from the two mentioned unloading events, which occur at the expansion onset, a considerable amount of energy input was continuously used from 11:35 UT until 12:40 UT for the growth of the directly driven system.

The method presented here estimates the energy changes in the inner magnetosphere-ionosphere system during a magnetospheric substorm. We have made an effort to define a more appropriate energy function for the output magnetospheric energy in order to have a more realistic approach in the description of the energy budget of the magnetosphere-solarwind system. We expect that the gross features obtained from this analysis are valid, since most of them are in accordance with the results obtained from the analysis of the magnetotail and ground data.

Acknowledgements. The authors are grateful to C. T. Russell for providing the ISEE magnetic field data and to J. Dandouras for providing the ISEE energy flux data. Thanks are also due to Mrs P. Tatsi for technical help.

Editor-in-chief, S. W. H. Cowley thanks three referees for their help in evaluating this paper.

References

Akasofu, S.-I., The solar wind-magnetosphere energy coupling and magnetospheric disturbances, *Planet. Space Sci.*, **28,** 495–509, 1980.

Akasofu, S.-I., Energy coupling between the solar wind and the magnetosphere, *Space Sci. Rev.*, **28,** 121–190, 1981.

Alfven, H., Cosmic Plasma, *Astrophys. Space Sci. Library*, **82,** D. Reidel Publ. Co., Dordrecht, 1891.

Anderson, K. A., R. P. Lin, R. J. Paoli, G. K. Parks, C. S. Lin, H. Reme, J. M. Bosqued, F. Martel, F. Coten, and A. Cross, An experiment to study energetic particle fluxes in and beyond the earth's outer magnetosphere, *IEEE Trans. Geosci. Electron.*, **GE-16,** 213–216, 1978.

Burton, R. K., R. L. McPherron, and C. T. Russell, An empirical relationship between interplanetary conditions and D_{st}, *J. Geophys. Res.*, **80,** 4204–4214, 1975.

Camidge, F. P., and G. Rostoker, Magnetic field perturbations in the magnetotail associated with the polar magnetic substorms, *Can. J. Phys.*, **48,** 2002–2010, 1970.

Chao, J. K., J. R. Kan, A. T. Y. Lui, and S.-I. Akasofu, A model for thinning of plasma sheet, *Planet. Space Sci.*, **25,** 703–710, 1977.

Clauer, C. R., R. L. McPherron, and C. Searls, Solar wind control of the low-latitude asymmetric magnetic disturbance field, *J. Geophys. Res.*, **88,** 2123–2130, 1983.

Fairfield, D. H., and N. F. Ness, Configuration of the geomagnetic tail during substorms, *J. Geophys. Res.*, **75,** 7032–7047, 1970.

Fairfield, D. H., R. P. Lepping, E. W. Hones, Jr., S. J. Bame, and J. R. Asbridge, Simultaneous measurements of magnetotail dynamics by IMP spacecraft, *J. Geophys. Res.*, **86,** 1396–1414, 1981.

Hones, E. W. Jr., J. R. Asbridge, S. J. Bame, and S. Singer, Substorm variations of the magnetotail plasma sheet from $X_{SM} = -6R_E$ to $X_{SM} = -60R_E$, *J. Geophys. Res.*, **78,** 109–132, 1973.

Hones, E. W. Jr., T. Pytte, and H. I. West, Jr., Associations of geomagnetic activity with plasma sheet thinning and expansion: a statistical study, *J. Geophys. Res.*, **89,** 5471–5478, 1984.

Kamide, Y., and S.-I. Akasofu, Latitudinal cross section of the auoral electrojet and its relation to the interplanetary magnetic field polarity, *J. Geophys. Res.*, **79,** 3755–3771, 1974.

Kan, J. R., and S.-I. Akasofu, A model of the open magnetosphere, *J. Geophys. Res.*, **79,** 1379–1384, 1974.

Kaufmann, R. L., Substorm currents: Growth and onset, *J. Geophys. Res.*, **92,** 7471–7486, 1987.

Kokubun, S., and R. L. McPherron, Substorm signatures at synchronous altitude, *J. Geophys. Res.*, **86,** 11265–11277, 1981.

Kropotkin, A. P., On the physical mechanism of the magnetospheric substorm development, *Planet. Space Sci.*, **20,** 1245–1257, 1972.

Lopez, R. E., and A. T. Y. Lui, A multisatellite case study of the expansion of a substorm current wedge in the near-earth magnetotail, *J. Geophys. Res.*, **95,** 8009–8017, 1990.

Lui, A. T. Y., Estimates of current changes in the magnetotail associated with a substorm, *Geophys. Res. Lett.*, **5,** 853–856, 1978.

Lui, A. T. Y., A synthesis of magnetospheric substorm models, *J. Geophys. Res.*, **96,** 1849–1856, 1991.

Lui, A. T. Y., R. E. Lopez, S. M. Krimigis, R. W. McEntire, L. J. Zanetti, and T. A. Potemra, A case study of magnetotail current sheet disruption and diversion, *Geophys. Res. Lett.*, **15,** 721–724, 1988.

Mavromichalaki, H., and A. Belehaki, Mechanisms and time-scales of the magnetospheric response to the interplanetary magnetic field changes during the May 8th, 1986, *J. Atmosph. Terr. Phys.*, **55,** 1459–1467, 1993.

McPherron, R. L., CDAW-9 Event E: evidence for a near-Earth neutral line, *Proc. IUGG XX Assembly*, IAGA Abstracts, 438, 1991.

McPherron, R. L., M. P. Aubry, C. T. Russell, and J. P. Coleman, Jr., Satellite studies of magnetospheric substorms on August 15, 1968, 4. Ogo 5 magnetic field observations, *J. Geophys. Res.*, **78,** 3068–3078, 1973.

McPherron, R. L., D. Baker, R. Clauer, J. Craven, T. Eastman, D. Fairfield, W. Heikkila, N. Heiniman, E. Hones, T. Lui, R. Manka, G. Rostoker, H. Singer, and T. Sakurai, A multiple onset substorm during weak solar wind coupling: CDAW-9 evidence for a near-Earth neutral line, *Proc. AGU Fall Meeting*, **EOS 71,** 43, 1533, 1990.

Nagai, T., Observed magnetic substorm signatures at synchronous altitude, *J. Geophys. Res.*, **87,** 4405–4417, 1982.

Perreault, P., and S.-I. Akasofu, A study of geomagnetic storms, *Geophys. J. R. Astron. Soc.*, **54,** 547–573, 1978.

Pytte, T., R. L. McPherron, E. W. Hones, Jr., and H. I. West, Jr., Multiple-satellite studies of magnetospheric substorms: distinction between polar magnetic substorms and convection-driven negative bays, *J. Geophys. Res.*, **83,** 663–679, 1978.

Rostoker, G., S.-I. Akasofu, J. Foster, R. A. Greenwald, Y. Kamide, K. Kawasaki, A. T. Y. Lui, R. L. McPherron, and C. T. Russell, Magnetospheric substorms – definition and signatures, *J. Geophys. Res.*, **85,** 1663–1668, 1980.

Rostoker, G., S.-I. Akasofu, W. Baumjohann, Y. Kamide, and R. L. McPherron, The roles of direct input of energy from the solar wind and unloading of stored magnetotail energy in driving magnetospheric substorms, *Space Sci. Rev.*, **46,** 93–111, 1987.

Russell, C. T., The ISEE-1 and 2 fluxgate magnetometers, *IEEE Trans. Geosci. Electron.*, **GE-16,** 239–242, 1978.

Saifudinova, T. I., A. D. Bazarzhapov, D.Sh. Shirapov, S. B. Lunyushkin, and V. M. Michin, Substorm scenario with two active phases: A study of CDAW-9-E events, *Proc. Int. Conf. Substorms (ICS-1)*, Kiruna, Sweden, 391–395, 1992.

Sauvaud, J.-A., and J.R. Winckler, Dynamics of plasma, energetic particles, and fields near synchronous orbit in the night-time sector during magnetospheric substorms, *J. Geophys. Res.*, **85,** 2043–2056, 1980.

Vasyliunas, V. M., A method for evaluating the total magnetospheric energy output independently of the ε parameter, *Geophys. Res. Let.*, **14,** 1183–1186, 1987.

Zwickl, R. D., L. F. Bargatze, D. N. Baker, C. R. Clauer, and R. L. McPherron, An evaluation of the total magnetospheric energy output parameter, U_T, in: *Magnetotail Physics*, Ed A. T. Lui, The Johns Hopkins University Press, Baltimore, 155–159, 1987.